


3D geometric morphometric analysis of the distal radius insertion sites of the palmar radiocarpal ligaments indicates a relationship between wrist anatomy and unique locomotor behavior in hylobatids

Aroa Casado^{1,2} | Elisabeth Cuesta-Torralvo² | Juan Francisco Pastor³ |
Marina De Diego¹ | Mónica Gómez¹ | Neus Ciurana¹ | Josep Maria Potau^{1,2} 

¹Unit of Human Anatomy and Embryology, University of Barcelona, Barcelona, Spain

²Institut d'Arqueologia de la Universitat de Barcelona (IAUB), Faculty of Geography and History, University of Barcelona (UB), Barcelona, Spain

³Department of Anatomy and Radiology, University of Valladolid, Valladolid, Spain

Correspondence

José Maria Potau, Unit of Human Anatomy and Embryology, University of Barcelona, C/Casanova 143, 08036 Barcelona, Spain.
Email: jpotau@ub.edu

Funding information

European Union, Grant/Award Number: CGL2014-52611-C2-2-P; Ministerio de Economía y Competitividad; Universitat de Barcelona, Grant/Award Number: APIF-UB 2016/2017

Abstract

Objectives: The objective of this study is to explore the anatomical differences in the insertion sites of the palmar radiocarpal ligaments between hylobatids and other hominoids that may be related to their different locomotor behaviors.

Materials and Methods: The morphology of the insertion sites of the palmar radiocarpal ligaments was analyzed with three-dimensional geometric morphometrics (3D GM) in the distal radial epiphysis of 44 hylobatids, 25 *Pan*, 31 *Gorilla* and 15 *Pongo*.

Results: Relative to other hominoids, hylobatid insertion sites of the palmar radiocarpal ligaments were relatively larger and the insertion site of the short radiolunate ligament had a palmar orientation.

Discussion: Larger palmar radiocarpal ligaments in hylobatids can help stabilize the wrist during the radial and ulnar displacement that occurs in ricochet brachiation, the characteristic locomotor behavior of hylobatids, and compensate for the large traction loads on the wrist during extended-elbow vertical climbing.

KEYWORDS

distal radius, hominoid primates, hylobatids, radiocarpal ligaments

1 | INTRODUCTION

The primates of the family Hylobatidae have marked morphological differences from the other primates in the superfamily Hominoidea (Schultz, 1933). Hylobatidae comprises the genera *Nomascus*, *Hylobates*, *Hoolock* and *Symphalangus*, which are genetically differentiated (Carbone et al., 2014). These genera have a wide variety of locomotor behaviors, including quadrupedal walking and jumping (Vereecke et al., 2006) and three forms of arboreal locomotion (vertical climbing, orthograde clambering, and brachiation), with brachiation being the most common (Fan et al., 2013; Fleagle, 1976). In addition, they can use a wide variety of other locomotor modes, such as diving, bridging, bipedal walking, running, quadrumanous climbing, and scrambling (Vereecke et al., 2006).

One of the most striking anatomical features of the hylobatids is their long upper limb relative to a small body size (Schultz, 1933; Takahashi, 1990; Zihlman et al., 2011), which permits a suspensory locomotion that is kinematically different from that of other hominoid and non-hominoid primates (Hunt, 1991; Isler, 2005). The brachiation practiced by hylobatids is characterized by a high biomechanical efficiency, short cycles, a high transfer rate between movements, and asymmetrical cycles in the use of the lower limbs (Isler, 2002). Together, these characteristics lead to a concentration in the upper limb of virtually all the work factor generated during brachiation (Thorpe & Crompton, 2006). In turn, this produces a series of traction forces that necessitate morphological changes in the upper limb and the wrist to stabilize the radial and ulnar deviation that takes place

This is an open access article under the terms of the [Creative Commons Attribution-NonCommercial-NoDerivs](https://creativecommons.org/licenses/by-nc-nd/4.0/) License, which permits use and distribution in any medium, provided the original work is properly cited, the use is non-commercial and no modifications or adaptations are made.

© 2022 The Authors. *American Journal of Biological Anthropology* published by Wiley Periodicals LLC.

(Sarmiento, 1988). Another differential anatomical characteristic of hylobatids is hypertrophy of the proximal muscles of the upper limb (Michilsens et al., 2009), coupled with a relatively smaller distal muscle mass. This anatomical configuration makes it possible to achieve a smooth rolling movement during brachiation, since the non-supporting limb can swing quickly and easily up to the next handgrip (Michilsens et al., 2009). Finally, in contrast to other hominoids, hylobatids can more easily move their center of body mass by flexing or extending their elbow, thus enhancing the pendulum effect of the body during contact with the handgrip and improving their speed (Michilsens et al., 2009).

The anatomical peculiarities of the upper limb of hylobatids have been explored over the past few years from both an osteological (Orr, 2017; Prime & Ford, 2016; Richmond et al., 2001) and a muscular (Van Leeuwen et al., 2018; Vanhoof et al., 2020) perspective. However, few studies have quantitatively examined the functional adaptations of the upper limb of hylobatids in relation to their locomotor behavior (Michilsens et al., 2009; Vanhoof et al., 2020).

Unlike other osteological regions of the upper limb, the distal radial epiphysis has no well-defined muscle insertion sites to link its morphological differences with the locomotor behaviors developed by hominoids. However, in the distopalmar region of the distal radial epiphysis, the insertion sites of the main ligaments that stabilize the radiocarpal joint can be observed (Casado et al., 2019; Figure 1). Specifically, a common insertion site for the radioscapocapitate (RSC) and long radiolunate (LRL) ligaments and an insertion site for the short

radiolunate (SRL) ligament can be identified. The RSC ligament connects the palmar surface of the styloid process of the radius with the scaphoid and the capitate bone (Buijze et al., 2011). Its main function is to stabilize the scaphoid (Apergis, 2013; Ringler & Murthy, 2015). The LRL ligament connects the palmar surface of the scaphoid fossa of the radius with the lunate bone, and the SRL ligament connects the palmar surface of the lunate fossa of the radius with the lunate bone (Ringler & Murthy, 2015). The main function of the LRL and SRL is to stabilize the lunate bone (Apergis, 2013; Ringler & Murthy, 2015). The morphology of these insertion sites can be related to the functional characteristics of the wrist of hominoids and their locomotor behavior (Casado et al., 2019). The more terrestrial hominoids, such as gorillas, are characterized by relatively small insertion sites, with an ulnopalmar orientation of the SRL insertion site (Casado et al., 2019), which is related to their osteological morphology. This morphology provides greater stability of the scaphoid and the lunate and reduced mobility of the wrist, which in turn reduces the need for the ligaments to provide stability (Orr, 2017). In contrast, the more arboreal hominoids, such as chimpanzees or orangutans, have relatively large insertion sites and a palmar orientation of the SRL insertion site (Casado et al., 2019). This relatively larger size of the radiocarpal ligaments is related to their use of arboreal locomotion, since these ligaments compensate for the large traction loads on the wrist during suspensory locomotion and vertical climbing (Richmond et al., 2001).

Based on these previous findings in other hominoid taxa, in this study we analyze the insertion sites of the palmar radiocarpal

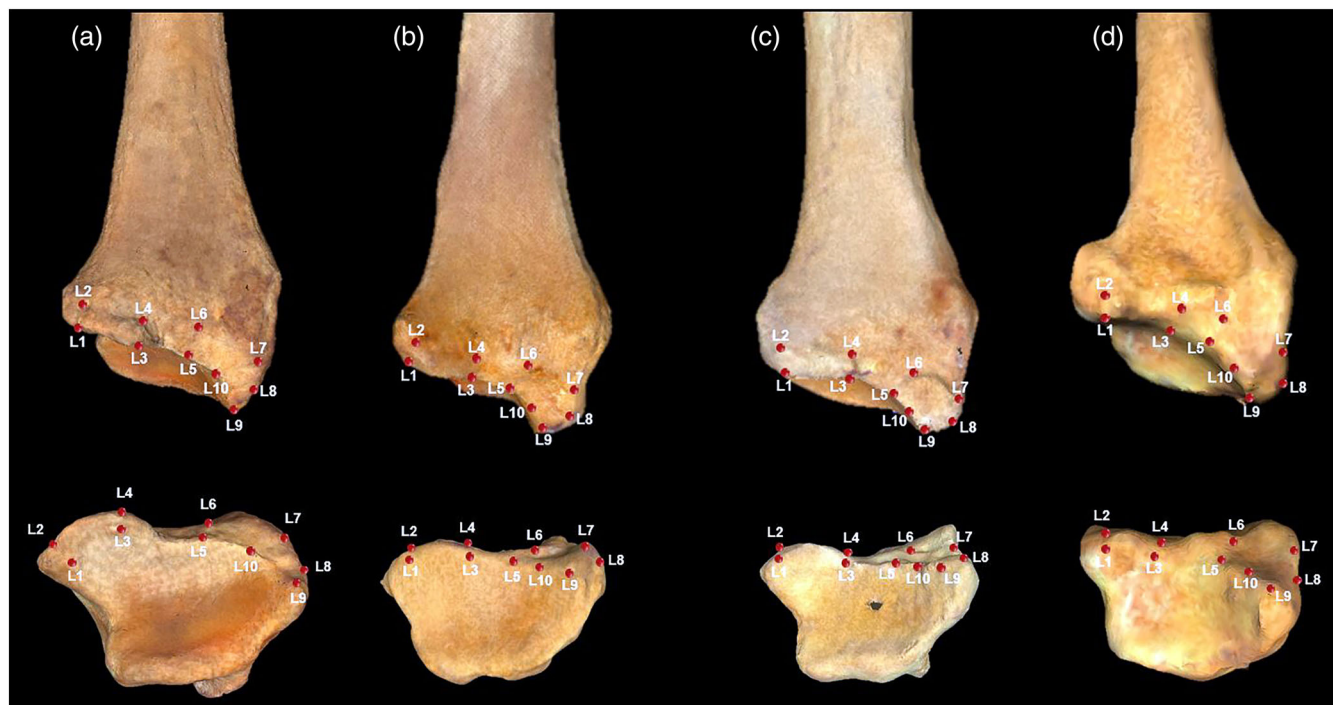


FIGURE 1 Distal radial epiphyses of (a) *Gorilla gorilla*, (b) *Pan troglodytes*, (c) *Pongo pygmaeus* and (d) *Hylobates lar*, in a palmar view (upper panel) and a distal view (lower panel). In each of the distal radial epiphyses, the insertion sites of the palmar radiocarpal ligaments are shown with the locations of the landmarks. Landmarks L1-L4 identify the SRL ligament insertion site, and landmarks L5-L10 identify the RSC + LRL ligaments insertion site. LRL, long radiolunate; RSC, radioscapocapitate; SRL, short radiolunate.

ligaments of hylobatids using three-dimensional geometric morphometrics (3D GM) with the aim of determining whether their characteristic morphology can be quantitatively differentiated from that of other hominoids and whether it is related to their unique locomotor behavior. The results obtained from this study can help to increase the currently available knowledge of the anatomy and wrist function of hylobatids, especially at the osteological and ligamentous level, and may help inform behavioral reconstructions of fossil hominoids.

2 | MATERIALS AND METHODS

2.1 | Osteological samples

A total of 115 left radii (Table 1) belonging to *Pan troglodytes* ($N = 25$), *Gorilla gorilla* ($N = 31$), *Pongo pygmaeus* ($N = 12$), *Pongo abelii* ($N = 3$), *Hylobates lar carpenteri* ($N = 26$), *Symphalangus syndactylus* ($N = 9$), *Hylobates moloch* ($N = 4$), *Hylobates pileatus* ($N = 2$), *Hoolock hoolock* ($N = 1$), and *Hylobates muelleri* ($N = 2$) were analyzed in this study. All the specimens came from the *Anthropologisches Institut und Museum* (AIM) of the University of Zurich, Switzerland and correspond to adult individuals who died from reasons unrelated to this study. All specimens used in this study were wild-shot and did not present macroscopic pathology. The adult age of the specimens was estimated by dental eruption patterns and the total fusion of the distal radial epiphysis.

2.2 | 3D GM analysis

The distal radial epiphysis of each specimen was scanned by a 3D Next Engine Ultra HD laser surface scanner, at a resolution of 0.1 mm space-point separation with a density of 40 k (2x) points. The different sections of the scans were fused with the Volume Merge option of Next Engine HD software at a resolution of 0.5 mm and saved as a

TABLE 1 Osteological samples used in the 3D GM analysis. UZH = University of Zurich. **Pan* included one individual of unknown sex

Total sample	N	Male	Female	Collection
Gorilla gorilla	31	17	14	UZH
Pan troglodytes	25*	11	13	UZH
Pongo pygmaeus	12	7	5	UZH
Pongo abelii	3	1	2	UZH
Hylobates lar carpenteri	26	13	13	UZH
Symphalangus syndactylus	9	4	5	UZH
Hylobates moloch	4	2	2	UZH
Hylobates pileatus	2	2	–	UZH
Hoolock hoolock	1	1	–	UZH
Hylobates muelleri	2	2	–	UZH
Total	115	60	54	

PLY file. The resulting triangle mesh was edited with the open-source MeshLab software (Cignoni et al., 2008) and the models were imported into Landmark Editor software (v. 3.6) (Wiley, 2006) for placing the landmarks (Casado et al., 2019).

The sets of landmarks proposed by Casado et al. (2019) (Table 2) were used to represent the morphology of the two insertion sites of the palmar radiocarpal ligaments in the distal radial epiphysis (Figure 1). Ten type III landmarks were used: the L1-L4 landmarks for the SRL insertion site and the L5-L10 landmarks for the common insertion site of the RSC and LRL. The raw data obtained with Landmark Editor software based on the landmark coordinates were exported into the MorphoJ statistical package (Klingenberg, 2011).

In order to confirm the reliability and reproducibility of the landmarks, we calculated intra- and inter-observer error before beginning the 3D GM analysis. Three experienced investigators each placed all the landmarks in the 44 hylobatids specimens on three separate days, with a 48-h interval between the days to decrease the possibility of an investigator mechanically repeating the placement of the landmarks. Observer error in the other specimens had been calculated in a previous study by our group (Casado et al., 2021). Differences were analyzed with a pairwise Mann–Whitney analysis to detect any lack of reliability in the landmarks or the data.

A generalized Procrustes analysis (GPA) was used to eliminate variability due to differences of size, placement, or orientation and to minimize the sum of square distances between equivalent landmarks (Bookstein, 1991; O'Higgins, 2000; Zelditch et al., 2004). This procedure allows the resulting data, termed Procrustes coordinates, to be

TABLE 2 Numbering, description and types of landmarks used in the 3D GM analysis (O'Higgins, 2000)

Landmark	Type	Description
1	II	Most distal-ulnar point of the SRL ligament insertion area
2	II	Most proximal-ulnar point of the SRL ligament insertion area
3	II	Most distal-radial point of the SRL ligament insertion area
4	II	Most proximal-radial point of the SRL ligament insertion area
5	II	Most distal-ulnar point of the RSC + LRL ligaments insertion area
6	II	Most proximal-ulnar point of the RSC + LRL ligaments insertion area
7	II	Most proximal-radial point of the RSC + LRL ligaments insertion area
8	II	Most radial point of the RSC + LRL ligaments insertion area
9	II	Most distal-radial point of the RSC + LRL ligaments insertion area
10	III	Intermediate point between landmarks 5 and 9

Abbreviations: LRL, long radiolunate; RSC, radioscapocapitate; SRL, short radiolunate.

used in a multivariate analysis (Rohlf & Marcus, 1993; Zelditch et al., 2004). A principal components analysis (PCA) was then performed in order to reduce complex multidimensional data to fewer components, or eigenvectors, which could be used to explain the main differences between the groups (Klingenberg, 2011; O'Higgins, 2000; Zelditch et al., 2004). Subsequently, the normality of the sample was tested using the Shapiro–Wilk and Anderson–Darling tests in PAST software. Multivariate analyses of the variance (MANOVA and PERMANOVA) were performed to explore the observed differences between all major components and determine their potential statistical significance. Differences between males and females were explored at the genus level with the Mann–Whitney U and T tests, but we did not include species with no male or no female specimens.

In order to determine the influence of size on variation in shape (allometric scaling), a multivariate regression analysis (MRA) was performed with the PC1 as the dependent variable and the logarithm of the centroid size as the independent variable (Bookstein, 1991; Klingenberg, 2011; O'Higgins, 2000; Zelditch et al., 2004).

For more robust results to complement those obtained with the 3D GM analysis, we used the 3D scans of the distal radial epiphysis to obtain quantitative data on the ligament insertion sites. We used

MeshLab to calculate the surface area of the insertion site of the RSC + LRL ligaments in mm^2 and we normalized these values relative to the surface area of the distal articular surface of the radius.

2.3 | Ethical note

The research complied with protocols approved by the Institutional Animal Care and Use Committee of the University of Barcelona and adhered to the legal requirements of Spain.

3 | RESULTS

The analyses of intra- and inter-observer error revealed no significant differences (Table S1). The PCA identified 23 principal components (PCs), the first six of which explained 74.58% of the variation in shape of the two insertion sites of the palmar radiocarpal ligaments (PC1, 32%; PC2, 12.6%; PC3, 11.03%; PC4, 7.7%; PC5, 5.83%; PC6, 5.42%). The remaining PCs accounted for <5% each of the variation in shape. The scatterplot of PC1 versus PC2 (Figure 2) shows the differences

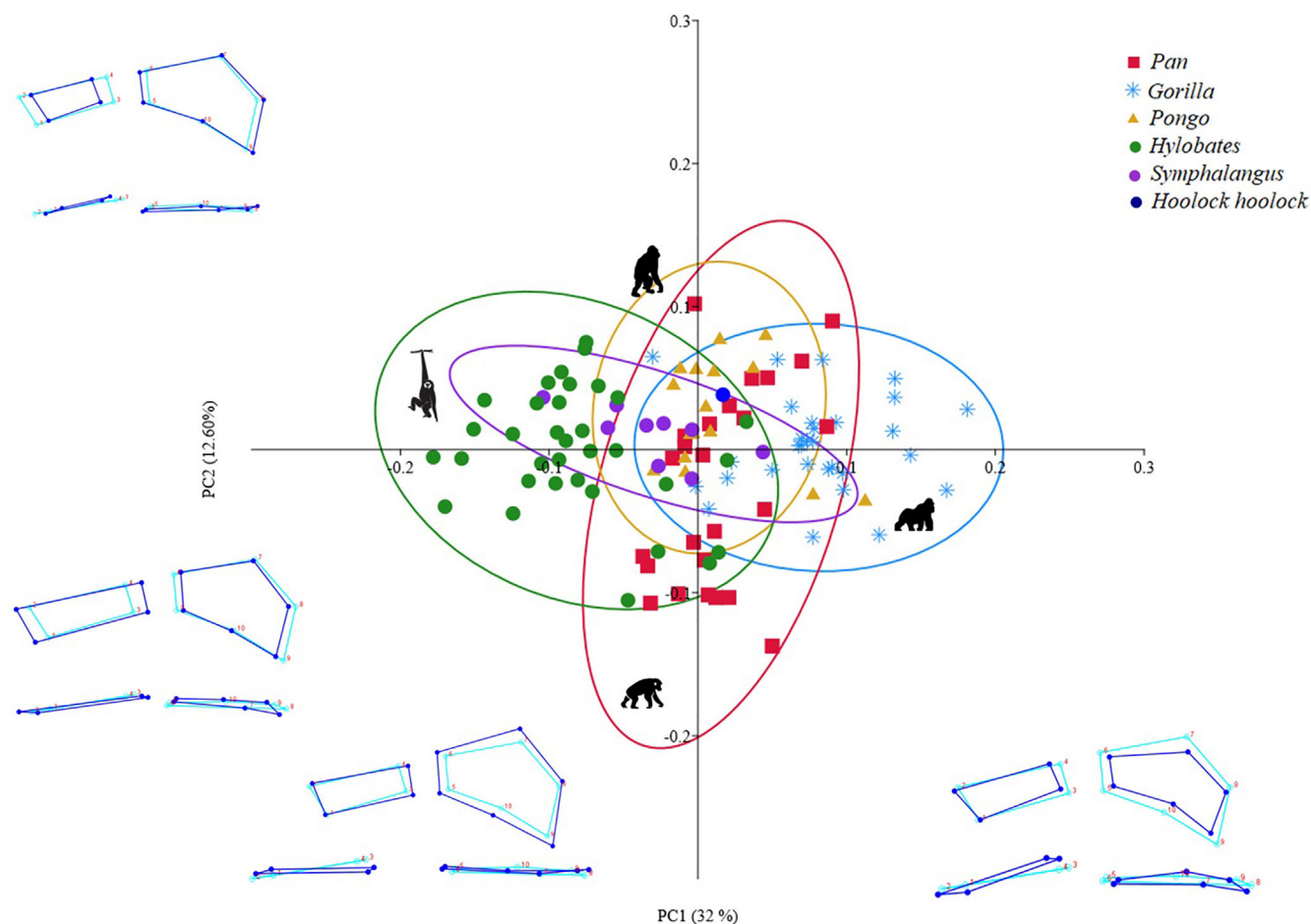


FIGURE 2 Scatter plot of PC1 versus PC2 derived from the PCA of the 3D GM analysis. 95% equal frequency ellipses of the groups are depicted. Dark blue wireframes show the extreme shape of each PC in a palmar view (upper panel) and a distal view (lower panel). Light blue wireframes show the mean shape (coordinates 0.0). 3S GM, three-dimensional geometric morphometrics; PCA, principal components analysis.

among the groups studied, although there is a high degree of overlap between groups. The hylobatids are located in the negative PC1 values, with members of the genus *Symphalangus* having more positive values than those of the genus *Hylobates*. Within the group of *Hylobates*, there is a separate cluster comprising four specimens (Figure 2); this cluster has no taxonomic significance since it is made up of three *Hylobates lar* and one *Hylobates pileatus*. *Gorilla* is located in the positive PC1 values, and *Pan* and *Pongo* are located near the 0.0 PC1 value. PC2 does not show large differences between the four groups of hominoids, nor do PC3 or PC4 (Figures S1 and S2).

The PC1 findings (Figure 2) showed that specimens with positive PC1 values were characterized by a relatively small insertion site of the RSC + LRL ligaments and by an ulnopalmar orientation of the SRL insertion site (Figure 1). In contrast, in specimens with negative PC1 values, the RSC + LRL insertion site was relatively large and the SRL insertion site had a palmar orientation (Figure 1). The MANOVA analysis for PCs with parametric distribution (PCs 1, 3, 5–8, 10–15, 17–20, 22, and 23) identified significant differences between hylobatids (including *Symphalangus*) and the other hominoids ($F: 6.1; p < 0.001$). The PERMANOVA analysis for PCs with non-parametric distribution (PCs 2, 4, 9, 16, and 21) also identified significant differences between hylobatids and the other hominoids ($F: 8.6; p < 0.001$), except in the case of the PC2 for *Gorilla* ($p = 0.20$). There were no significant differences in PC1 between males and females in any of the groups studied (*Gorilla* $U = 80, p = 0.13$; *Pan* $U = 69, p = 0.91$; *Pongo* $F = 1.18, p = 0.29$; *Hylobates* $U = 111, p = 0.23$; *Symphalangus* $F = 0.36, p = 0.35$).

The MRA of PC1 on the logarithm of the centroid size indicated that 68.10% of the variation in the shape of the insertion sites of the palmar radiocarpal ligaments was attributable to size ($p < 0.001$). The quantitative analysis of the RSC + LRL insertion site normalized to the distal articular surface of the radius (Table 3) showed significantly

higher values in *Hylobates* than in *Pan troglodytes* (0.35 vs. 0.25; $p = 0.0001$), *Gorilla gorilla* (0.35 vs. 0.27; $p = 0.05$), and *Pongo pygmaeus* (0.35 vs. 0.27; $p = 0.032$). Higher values were also observed in *Symphalangus* than in the other hominoids but the difference was only significant when comparing *Symphalangus* with *Pan troglodytes* (0.34 vs. 0.25; $p = 0.02$) but not with *Gorilla gorilla* (0.34 vs. 0.27; $p = 0.99$) or *Pongo pygmaeus* (0.34 vs. 0.27; $p = 0.18$). There were no significant differences between *Symphalangus* and *Hylobates* (0.34 vs. 0.35; $p = 0.607$) in the RSC + LRL insertion site normalized to the distal articular surface of the radius.

4 | DISCUSSION

The main finding of our 3D GM analysis is the separation of most *Hylobates* from the other hominoids. *Hylobates* had negative PC1 values (Figure 2), indicating a relatively large RSC + LRL insertion site. This finding is in line with the results of our quantitative analysis, which indicated that the RSC + LRL insertion site in hylobatids was larger than in the other hominoids (Table 3). This larger insertion site may be the result of osteological modifications in the radiocarpal joint of *Hylobates*, primarily in the scaphoid and lunate bones. *Hylobates* have a relatively small scaphoid with a relatively large lunate facet, which gives them more wrist mobility (Kivell et al., 2013). In addition, their lunate bone is proximodistally shorter and mediolaterally narrower than that of other arboreal primates, with a smaller radial facet and a larger scaphoid facet (Kivell et al., 2013). These osteological differences could explain the need for a greater development of the palmar radiocarpal ligaments, since these ligaments limit the extension and ulnar deviation of the wrist and are fundamental in the stabilization of the scaphoid (by the RSC) and lunate (by the LRL; Apergis, 2013; Bateni et al., 2013; Cardoso & Szabo, 2007; Nordin & Frankel, 2001; Ringler & Murthy, 2015; Short et al., 2002; Short et al., 2007). In addition, *Hylobates* had a palmar—rather than ulnopalmar—orientation of the SRL insertion site (Figure 1). The SRL is functionally important since it limits the extension and ulnar deviation of the wrist and stabilizes the lunate bone (Apergis, 2013; Short et al., 2002; Short et al., 2007).

However, the allometric scaling of 68.10% on the PC1, where the largest interspecific differences were detected, indicates that the differences observed in the 3D GM analysis in the insertion sites of the palmar radiocarpal ligaments may well be related to the size of the individuals analyzed. The separation on PC1 of most hylobatids from the other hominoids may reflect the smaller body size of the hylobatids. This smaller body size has enabled the hylobatids to develop their own specific locomotor behavior (Cartmill, 1985), which can account for the morphological characteristics that we have observed in the insertion sites of the palmar ligaments of the wrist. Hylobatids combine safer locomotor behavior, such as brachiation and vertical climbing (Chatani, 2003; Thorpe & Crompton, 2005), with ricochetal brachiation, arm swinging, and more dangerous aerial phases (Fan et al., 2013; Orr, 2017). This characteristic locomotor behavior is made possible by the combination of a small body size

TABLE 3 Mean, standard deviations (in parenthesis), and statistical significance of the quantitative analysis of the surface area of the insertion site of the RSC + LRL ligaments normalized to the surface area of the distal articular surface (DAS) of the radius

	RSC + LRL/DAS
Hylobates vs. <i>Pan troglodytes</i>	0.35 (0.11) vs. 0.25 (0.8) $p = 0.0001$
Hylobates vs. <i>Gorilla gorilla</i>	0.35 (0.11) vs. 0.27 (0.10) $p = 0.05$
Hylobates vs. <i>Pongo pygmaeus</i>	0.35 (0.11) vs. 0.27 (0.08) $p = 0.032$
<i>Symphalangus</i> vs. <i>Pan troglodytes</i>	0.34 (0.11) vs. 0.25 (0.8) $p = 0.02$
<i>Symphalangus</i> vs. <i>Gorilla gorilla</i>	0.34 (0.11) vs. 0.27 (0.10) $p = 0.99$
<i>Symphalangus</i> vs. <i>Pongo pygmaeus</i>	0.34 (0.11) vs. 0.27 (0.08) $p = 0.18$
Hylobates vs. <i>Symphalangus</i>	0.35 (0.11) vs. 0.34 (0.11) $p = 0.607$

Abbreviations: LRL, long radiolunate; RSC, radioscapocapitate.

(Schultz, 1933; Zihlman et al., 2011) with a characteristic morphology of hominoids: a shortened lumbar region, a dorsoventral flattening and lateral expansion of the thorax (Selby & Lovejoy, 2017), a dorsally repositioned and craniocaudally elongated scapula, and a shortened olecranon that facilitates elbow extension (Byron et al., 2017). In addition, hylobatids have their own unique anatomical adaptations: thin, hook-shaped hands with extremely long fingers; a unique ball-and-socket wrist joint; particular muscle characteristics, such as powerful elbow flexors; and an extremely long anterior limb (Isler, 2005) that decreases the specific metabolic cost of mass per unit distance traveled (Pontzer, 2007; Pontzer, 2016). This differentiated morphology makes it possible for hylobatids to rely on suspensory behaviors, with a significant proportion of aerial phases during arboreal locomotion (Cant et al., 2001; Cant et al., 2003). The use of brachiation in hylobatids ranges from 48% to 84% of total locomotion time, with quadrupedal locomotion being virtually non-existent, unlike other members of the hominoid superfamily (Cant et al., 2001; Gebo, 1996). Furthermore, several studies have found that the type of suspension used by hylobatids in the aerial phases is kinematically different from that of other primates (Fan et al., 2009; Usherwood et al., 2003), as hylobatids uses a ricochetal brachiation that includes a phase of true flight between contacts with the support elements (Chang et al., 2000; Prime & Ford, 2016). This type of brachiation involves both a rotation of the trunk and the complete extension of the supporting limb before the flight phase (Bertram & Chang, 2001) as well as a considerable radial and ulnar deviation of the wrist (Sarmiento, 1988). This deviation would then be compensated by a greater development of the palmar radiocarpal ligaments to stabilize the radiocarpal joint in a neutral position (Byron et al., 2017). In addition, the smaller body of the hylobatids permits the use of extended-elbow vertical climbing, which is characterized by a longer duration of the support phase and is mechanically more demanding than other types of vertical climbing (Isler & Thorpe, 2003). This use of extended-elbow vertical climbing could well explain the larger size of the insertion sites of the wrist ligaments in hylobatids, which would compensate for the traction forces generated in the wrist (Tamagawa et al., 2020). Finally, hylobatids are the only hominoids with suspensory behavior where the load falls exclusively on the upper limb, while other primates have either clambering-type suspensory locomotion, where all four limbs are called into play, or transfer locomotion, where the load is on the upper limb only 10%–15% of the time (Cant, 1987; Rein et al., 2015; Thorpe & Crompton, 2006).

The characteristic brachiation of hylobatids, with the greater involvement of the upper limb, means that large traction loads affect the radiocarpal joint over an extended period of time (Rein et al., 2015) and this could explain the larger size of the insertion sites of the palmar radiocarpal ligaments that we have observed in our PCA (Figure 2). During this type of brachiation, the upper limb is under great tension, but the joints are also subjected to strong compression forces related to muscle contraction, since the flexor muscles of the elbow and the wrist work against gravity while the extensor muscles, which are more developed, work with gravity (Michilens et al., 2009; Swartz et al., 1989). To compensate for this tension in the radiocarpal joint, the wrist will have great strength but a low range of motion, which will guarantee its stability (Michilens

et al., 2009). It is therefore likely that the larger size of the insertion sites of the palmar radiocarpal ligaments in hylobatids is due to their unique body morphology, which can support a locomotor behavior that is impossible for other hominoids with larger bodies. This morphological variance could thus be explained by the fact that brachiation is unworkable in large-bodied primates, since a large body would produce greater tension in the supporting limb during swinging, which would increase the risk of rupture (Fan et al., 2013). The slight difference in the PCA between *Hylobates* and *Symphalangus* (Figure 2), although without statistical significance, supports this argument. *Symphalangus* have a larger body and their locomotor behavior is primarily swinging brachiation (Fleagle, 1974), which would explain their slight tendency toward more positive PCA values than *Hylobates* and their overlapping values with *Gorilla* and the arboreal hominoids *Pongo* and *Pan*. In contrast, *Hylobates* have a smaller body and their locomotor behavior is primarily ricochetal brachiation with more effective aerial phases (Cheyne, 2011), which requires a more stable radiocarpal joint and larger palmar radiocarpal ligaments.

In conclusion, our 3D GM analysis has identified significant differences in the RSC + LRL and SRL insertion sites in hylobatids compared to other hominoids. We have seen that the morphology of these insertion sites in hylobatids is more similar to that of arboreal primates like *Pan* and *Pongo* than to that of more terrestrial primates like *Gorilla*. We have also observed that the particular shape of these insertion sites in hylobatids may well be related to their unique locomotor behavior and to their smaller body size. Nevertheless, the high degree of overlap among the different groups in the PCA limits the functional interpretation of the morphological differences in the ligament insertion sites and highlights the relative morphological similarity of the distal radial epiphysis in different hominoids. Furthermore, since there was a large allometric influence on the PC1 and since we were unable to access complete data on the body size of our specimens, we suggest that future studies with access to these data should include allometric analyses to further examine the relationship between the smaller body size of hylobatids and the morphology of the radiocarpal ligament insertion sites.

AUTHOR CONTRIBUTIONS

Aroa Casado: Conceptualization (equal); data curation (lead); formal analysis (equal); funding acquisition (lead); investigation (equal); methodology (equal); project administration (equal); resources (equal); software (equal); supervision (equal); validation (equal); visualization (equal); writing – original draft (lead). **Elisabeth Cuesta-Torralvo:** Conceptualization (supporting); data curation (supporting); formal analysis (equal); investigation (supporting); methodology (supporting); software (supporting); validation (supporting); visualization (supporting). **Juan Francisco Pastor:** Conceptualization (equal); data curation (supporting); formal analysis (supporting); investigation (supporting); methodology (equal); software (supporting); validation (equal); visualization (supporting). **Marina De Diego:** Conceptualization (supporting); data curation (supporting); formal analysis (equal); investigation (supporting); methodology (supporting); software (supporting); validation (supporting); visualization (supporting). **Mónica Gómez:** Conceptualization (supporting); data curation (supporting); formal analysis (equal); investigation (supporting); methodology (supporting); software

(supporting); validation (supporting); visualization (supporting). **Neus Ciurana:** Conceptualization (supporting); data curation (supporting); formal analysis (equal); investigation (supporting); methodology (supporting); software (supporting); validation (supporting); visualization (supporting). **Josep Maria G Potau:** Conceptualization (lead); data curation (lead); formal analysis (lead); funding acquisition (lead); investigation (lead); methodology (lead); project administration (lead); resources (lead); software (lead); supervision (lead); validation (lead); visualization (lead); writing – original draft (equal).

ACKNOWLEDGMENTS

The authors thank Marcia Poncé de León and Christoph P. E. Zollikofer (UZH) for their advice and their kindness in granting us access to the material under their care. This study was funded by the Spanish Ministerio de Economía y Competitividad (project CGL2014-52611-C2-2-P to Josep Maria Potau), by the European Union (FEDER), and by the Ajudes Predoctorals of the University of Barcelona (APIF-UB 2016/2017 to Aroa Casado). The authors also thank Renee Grupp for assistance in drafting the manuscript.

CONFLICT OF INTEREST

The authors declare no conflict of interest.

DATA AVAILABILITY STATEMENT

The data that support the findings of this study are available from the corresponding author upon reasonable request.

ORCID

Josep Maria Potau  <https://orcid.org/0000-0003-3387-8760>

REFERENCES

- Apergis, E. (2013). Wrist anatomy. In Emmanuel Apergis (Ed.), *Fracture-dislocations of the wrist* (pp. 7–41). Springer. https://doi.org/10.1007/978-88-470-5328-1_2
- Bateni, C. P., Bartolotta, R. J., Richardson, M. L., Mulcahy, H., & Allan, C. H. (2013). Imaging key wrist ligaments: What the surgeon needs the radiologist to know. *American Journal of Roentgenology*, 200, 1089–1095. <https://doi.org/10.2214/ajr.12.9738>
- Bertram, J. E. A., & Chang, Y. H. (2001). Mechanical energy oscillations of two brachiation gaits: Measurement and simulation. *American Journal of Physical Anthropology*, 113, 319–326. <https://doi.org/10.1002/ajpa.1088>
- Bookstein, F. L. (1991). *Morphometric tools for landmark data: Geometry and biology*. Cambridge University Press.
- Buijze, G. A., Lozano-Calderon, S. A., Strackee, S. D., Blankevoort, L., & Jupiter, J. B. (2011). Osseous and ligamentous scaphoid anatomy: Part I. A systematic literature review highlighting controversies. *Journal of Hand Surgery*, 36, 1926–1935. <https://doi.org/10.1016/j.jhsa.2011.09.012>
- Byron, C. D., Granatosky, M. C., & Covert, H. H. (2017). An anatomical and mechanical analysis of the douc monkey (*genus Pygathrix*), and its role in understanding the evolution of brachiation. *American Journal of Physical Anthropology*, 164, 801–820. <https://doi.org/10.1002/ajpa.23320>
- Cant, J. G. H. (1987). Positional behavior of female Bornean orangutans (*Pongo pygmaeus*). *American Journal of Primatology*, 12, 71–90. <https://doi.org/10.1002/ajp.1350120104>
- Cant, J. G. H., Youlatos, D., & Rose, M. D. (2001). Locomotor behavior of *Lagothrix lagotherica* and *Ateles belzebuth* in Yasuni National Park, Ecuador: General patterns and nonsuspensory modes. *Journal of Human Evolution*, 41, 141–166. <https://doi.org/10.1006/jhev.2001.0485>
- Cant, J. G. H., Youlatos, D., & Rose, M. D. (2003). Suspensory locomotion of *Lagothrix lagotherica* and *Ateles belzebuth* in Yasuni National Park, Ecuador: General patterns and nonsuspensory modes. *Journal of Human Evolution*, 44, 685–700. [https://doi.org/10.1016/S0047-2484\(03\)00060-5](https://doi.org/10.1016/S0047-2484(03)00060-5)
- Carbone, L., Alan Harris, R., Gnerre, S., Veeramah, K. R., Lorente-Galdos, B., Huddleston, J., Meyer, T. J., Herrero, J., Roos, C., Aken, B., Anacleiro, F., Archidiacono, N., Baker, C., Barrell, D., Batzer, M. A., Blancher, A., Bohrsen, C. L., Brameier, M., Campbell, M. S., ... Gibbs, R. A. (2014). Gibbon genome and the fast karyotype evolution of small apes. *Nature*, 513, 195–201. <https://doi.org/10.1038/nature13679>
- Cardoso, R., & Szabo, R. M. (2007). Wrist anatomy and surgical approaches. *Orthopedic Clinics of North America*, 38, 127–148. <https://doi.org/10.1016/j.jocl.2007.02.010>
- Cartmill, M. (1985). Climbing. In M. Hildebrand, K. F. Bramble, & D. B. W. Liem (Eds.), *Functional vertebrate morphology* (pp. 73–88). Belknap Press.
- Casado, A., Avia, Y., Llorente, M., Riba, D., Pastor, J. F., & Potau, J. M. (2021). Effects of captivity on the morphology of the insertion sites of the palmar radiocarpal ligaments in hominoid primates. *Animals*, 11, 1856. <https://doi.org/10.3390/ani11071856>
- Casado, A., Punsola, V., Gómez, M., de Diego, M., Barbosa, M., de Paz, F. J., Pastor, J. F., & Potau, J. M. (2019). Three-dimensional geometric morphometric analysis of the distal radius insertion sites of the palmar radiocarpal ligaments in hominoid primates. *American Journal of Physical Anthropology*, 170, 24–36. <https://doi.org/10.1002/ajpa.23885>
- Chang, Y. H., Bertram, J. E. A., & Lee, D. V. (2000). External forces and torques generated by the brachiating white-handed gibbon (*Hylobatids Lar*). *American Journal of Physical Anthropology*, 113, 201–216. [https://doi.org/10.1002/1096-8644\(200010\)113:2%3C201::AID-AJPA5%3E3.0.CO;2-S](https://doi.org/10.1002/1096-8644(200010)113:2%3C201::AID-AJPA5%3E3.0.CO;2-S)
- Chatani, K. (2003). Positional behavior of free-ranging Japanese macaques (*Macaca fuscata*). *Primates*, 44, 13–23. <https://doi.org/10.1007/s10329-002-0002-z>
- Cheyne, S. M. (2011). Gibbon locomotion research in the field: Problems, possibilities, and benefits for conservation. In K. D'Août (Ed.), *Primate locomotion: Linking field and laboratory research* (pp. 201–213). Springer.
- Cignoni, P., Callieri, M., Corsini, M., Dellepiane, M., Ganovelli, F., & Ranzuglia, G. (2008). MeshLab: An open-source mesh processing tool. In V. Scarano, R. de Chiara, & U. Erra (Eds.), *6th Eurographics Italian Chapter Conference* (pp. 129–136). The Eurographics Association.
- Fan, P., Jiang, X., & Tian, C. (2009). The critically endangered black crested gibbon *Nomascus concolor* on Wuliang Mountain, Yunnan: The function of different forest types for the gibbon's conservation. *Oryx*, 43, 203–208. <https://doi.org/10.1017/S0030605308001907>
- Fan, P., Scott, M. B., Fei, H., & Ma, C. (2013). Locomotion behavior of cao vit gibbon (*Nomascus nasutus*) living in karst forest in Bangliang nature reserve, Guangxi, China. *Integrative Zoology*, 8, 356–364. <https://doi.org/10.1111/j.1749-4877.2012.00300.x>
- Fleagle, J. G. (1974). The dynamics of the brachiating siamang (*Symphalangus syndactylus*). *Nature*, 248, 259–260.
- Fleagle, J. G. (1976). Locomotion and posture of the Malayan siamang and implications for hominoid evolution. *Folia Primatologica*, 26, 245–269. <https://doi.org/10.1159/000155756>
- Gebo, D. L. (1996). Climbing, brachiation, and terrestrial quadrupedalism: Historical precursors of hominid bipedalism. *American Journal of Physical Anthropology*, 101, 55–92. [https://doi.org/10.1002/\(sici\)1096-8644\(199609\)101:1%3C55::aid-ajpa5%3E3.0.co;2-c](https://doi.org/10.1002/(sici)1096-8644(199609)101:1%3C55::aid-ajpa5%3E3.0.co;2-c)
- Hunt, K. (1991). Positional behavior in the Hominoidea. *International Journal of Primatology*, 12, 95–118.
- Isler, K. (2002). Characteristics of vertical climbing in gibbons. *Evolutionary Anthropology*, 11, 49–52. <https://doi.org/10.1002/evan.10055>

- Isler, K. (2005). 3D-kinematics of vertical climbing in hominoids. *American Journal of Physical Anthropology*, 126, 66–81. <https://doi.org/10.1002/ajpa.10419>
- Isler, K., & Thorpe, S. K. (2003). Gait parameters in vertical climbing of captive, rehabilitant and wild Sumatran orang-utans (*Pongo pygmaeus abelii*). *Journal of Experimental Biology*, 206, 4081–4096.
- Kivell, T. L., Barros, A. P., & Smaers, J. B. (2013). Different evolutionary pathways underlie the morphology of wrist bones in hominoids. *BMC Evolutionary Biology*, 13, 229. <https://doi.org/10.1186/1471-2148-13-229>
- Klingenberg, C. P. (2011). MorphoJ: An integrated software package for geometric morphometrics. *Molecular Ecology Resources*, 11, 353–357. <https://doi.org/10.1111/j.1755-0998.2010.02924.x>
- Michilsens, F., Vereecke, E. E., D'Août, K., & Aerts, P. (2009). Functional anatomy of the gibbon forelimb: Adaptations to a brachiating lifestyle. *Journal of Anatomy*, 215, 335–354. <https://doi.org/10.1111/j.1469-7580.2009.01109.x>
- Nordin, M., & Frankel, V. H. (2001). *Basic biomechanics of the musculoskeletal system*. Lippincott Williams and Wilkins.
- O'Higgins, P. (2000). The study of morphological variation in the hominid fossil record: Biology, landmarks and geometry. *Journal of Anatomy*, 197, 103–120.
- Orr, C. M. (2017). Locomotor hand postures, carpal kinematics during wrist extension, and associated morphology in anthropoid primates. *Anatomical Record*, 300, 382–401. <https://doi.org/10.1002/ar.23507>
- Pontzer, H. (2007). Effective limb length and the scaling of locomotor cost in terrestrial animals. *Journal of Experimental Biology*, 210, 1752–1761. <https://doi.org/10.1242/jeb.002246>
- Pontzer, H. (2016). A unified theory for the energy cost of legged locomotion. *Biological Letters*, 12, 20150935. <https://doi.org/10.1098/rsbl.2015.0935>
- Prime, J. M., & Ford, S. M. (2016). Hand manipulation skills in hylobatids. In U. H. Reichard, C. Borelli, H. Hirohisa, & M. G. Nowak (Eds.), *Evolution of gibbons and Siamang* (pp. 269–289). Springer Science & Business Media.
- Rein, T. R., Harvati, K., & Harrison, T. (2015). Inferring the use of forelimb suspensory locomotion by extinct primate species via shape exploration of the ulna. *Journal of Human Evolution*, 78, 70–79. <https://doi.org/10.1016/j.jhevol.2014.08.010>
- Richmond, B. G., Begun, D. R., & Strait, D. S. (2001). Origin of human bipedalism: The knuckle-walking hypothesis revisited. *Yearbook of Physical Anthropology*, 44, 70–105. <https://doi.org/10.1002/ajpa.10019>
- Ringler, M. D., & Murthy, N. S. (2015). MR imaging of wrist ligaments. *Medical Clinics of North America*, 23, 367–391. <https://doi.org/10.1016/j.mric.2015.04.007>
- Rohlf, F. J., & Marcus, L. (1993). A revolution in morphometrics. *Trends in Ecology & Evolution*, 8, 129–132.
- Sarmiento, E. E. (1988). Anatomy of the hominoid wrist joint: Its evolutionary and functional implications. *International Journal of Primatology*, 9, 281–345.
- Schultz, A. H. (1933). Observations on the growth, classification and evolutionary specialization of gibbons and siamangs. *Human Biology*, 5, 385–428.
- Selby, M. S., & Lovejoy, C. O. (2017). Evolution of the hominoid scapula and its implications for earliest hominid locomotion. *American Journal of Physical Anthropology*, 162, 682–700. <https://doi.org/10.1002/ajpa.23158>
- Short, W. H., Werner, F. W., Green, J. K., & Masaoka, S. (2002). Biomechanical evaluation of ligamentous stabilizers of the scaphoid and lunate. *Journal of Hand Surgery*, 27, 991–1002. <https://doi.org/10.1053/jhsu.2002.35878>
- Short, W. H., Werner, F. W., Green, J. K., Sutton, L. G., & Brutus, J. P. (2007). Biomechanical evaluation of the ligamentous stabilizers of the scaphoid and lunate: Part III. *Journal of Hand Surgery*, 32, 297–309. <https://doi.org/10.1016/j.jhsa.2006.10.024>
- Swartz, S. M., Bertram, J. E. A., & Biewener, A. A. (1989). Telemetered in vivo strain analysis of locomotor mechanics of brachiating gibbons. *Nature*, 342, 270–272. <https://doi.org/10.1038/342270a0>
- Takahashi, L. K. (1990). Morphological basis of arm-swinging: Multivariate analyses of the forelimb of Hylobates and Ateles. *Folia Primatologica*, 54, 70–85.
- Tamagawa, T., Lundh, T., Shigetoshi, K., Nitta, N., Ushio, N., Inubushi, T., Shiino, A., Karlsson, A., Inoue, T., Mera, Y., Hino, K., Komori, M., Morikawa, S., Sawajiri, S., Naka, S., Honma, S., Kimura, T., Uchimura, Y., Imai, S., ... Zhang, X. (2020). Correlation between musculoskeletal structure of the hand and primate locomotion: Morphometric and mechanical analysis in prehension using the cross and triple ratios. *PLoS One*, 15, e0232397. <https://doi.org/10.1371/journal.pone.0232397>
- Thorpe, S. K. S., & Crompton, R. H. (2005). Locomotor ecology of wild orangutans (*Pongo pygmaeus abelii*) in the Gunung Leuser Ecosystem, Sumatra, Indonesia: A multivariate analysis using log-linear modelling. *American Journal of Physical Anthropology*, 127, 58–78. <https://doi.org/10.1002/ajpa.20151>
- Thorpe, S. K. S., & Crompton, R. H. (2006). Orangutan positional behavior and the nature of arboreal locomotion in Hominoidea. *American Journal of Physical Anthropology*, 131, 384–401. <https://doi.org/10.1002/ajpa.20422>
- Usherwood, J. R., Larson, S. G., & Bertram, J. E. A. (2003). Mechanisms of force and power production in unsteady ricochet brachiation. *American Journal of Physical Anthropology*, 120, 364–372. <https://doi.org/10.1002/ajpa.10133>
- Van Leeuwen, T., Vanhoof, M. J. M., Kerkhof, F. D., Stevens, J. M. G., & Vereecke, E. E. (2018). Insights into the musculature of the bonobo hand. *Journal of Anatomy*, 233, 328–340. <https://doi.org/10.1111/joa.12841>
- Vanhoof, J. M., van Leeuwen, T., & Vereecke, E. E. (2020). The forearm and hand musculature of semiterrestrial rhesus macaques (*Macaca mulatta*) and arboreal gibbons (*Fam. Hylobatidae*). Part I. Description and comparison of the muscle configuration. *Journal of Anatomy*, 237, 774–790. <https://doi.org/10.1111/joa.13222>
- Vereecke, E. E., D'Août, K., & Aerts, P. (2006). Locomotor versatility of the white-handed gibbon (*Hylobates lar*): A spatiotemporal analysis of the bipedal, tripod and quadrupedal gaits. *Journal of Human Evolution*, 50, 552–567. <https://doi.org/10.1016/j.jhevol.2005.12.011>
- Wiley, D. F. (2006). *Landmark editor 3.0*. IDAV, University of California <http://graphics.idav.ucdavis.edu/research/EvoMorph>
- Zelditch, M. L., Swiderski, D. L., Sheets, H. D., & Fink, W. L. (2004). *Geometric morphometrics for biologists: A primer*. Academic Press.
- Zihlman, A. L., Mootnick, A. R., & Underwood, C. E. (2011). Anatomical contributions to hylobatid taxonomy and adaptation. *International Journal of Primatology*, 32, 865–877. <https://doi.org/10.1007/s10764-011-9506-y>

SUPPORTING INFORMATION

Additional supporting information may be found in the online version of the article at the publisher's website.

How to cite this article: Casado, A., Cuesta-Torralvo, E., Pastor, J. F., De Diego, M., Gómez, M., Ciurana, N., & Potau, J. M. (2022). 3D geometric morphometric analysis of the distal radius insertion sites of the palmar radiocarpal ligaments indicates a relationship between wrist anatomy and unique locomotor behavior in hylobatids. *American Journal of Biological Anthropology*, 178(4), 647–654. <https://doi.org/10.1002/ajpa.24568>